Synrad3D Photon propagation and scattering simulation *

G. Dugan, D. Sagan
CLASSE, Cornell University, Ithaca, NY 14853 USA

Abstract

As part of the Bmad software library, a program called Synrad3D has been written to track synchrotron radiation photons generated in storage rings. The purpose of the program is primarily to estimate the intensity and distribution of photon absorption sites, which are critical inputs to codes which model the growth of electron clouds. Synrad3D includes scattering from the vacuum chamber walls using X-ray data from an LBNL database. Synrad3D can handle any planar lattice and a wide variety of vacuum chamber profiles.

INTRODUCTION

The Bmad software library[1] has been used very successfully at Cornell for modeling relativistic charged particles in storage rings and linacs. Associated with this library are a number of programs used for lattice design and analysis. Recently, a new program that uses the Bmad library, called Synrad3D, has been developed to track synchrotron radiation photons generated in storage rings and linacs.

The motivation for developing Synrad3D was to estimate the intensity and distribution of photon absorption sites, which are critical inputs to codes which model the growth of electron clouds. Synrad3D includes scattering from the vacuum chamber walls using X-ray data from an LBNL database[2]. Synrad3D can handle any planar lattice and a wide variety of vacuum chamber profiles.

In the following sections, the general approach used in Synrad3D will be described, and two examples of its use will be presented.

APPROACH

Synrad3D uses Monte Carlo techniques to generate photons based on the standard synchrotron radiation formulas for dipoles, quadrupoles and wigglers, in the lattice of an accelerator. Any planar lattice can be handled. The lattice can be specified using Bmad, MAD, or XSIF formats. Photons are generated with respect to the particle beam's closed orbit, so the effect of variations in the orbit can be studied. In a linear accelerator lattice, since there is no closed orbit, the orbit is calculated from the user supplied initial orbit. The particle beam size is also taken into account when generating the photon starting positions. The emittance needed to calculate the beam size can be supplied by the user or is calculated from the standard radiation synchrotron radiation formulas.

* Work supported by the US National Science Foundation (PHY-0734867) and Department of Energy (DE-FC02-08ER41538)

REFLECTIVITY MODEL

Photons are tracked to the wall, where the probability of being scattered is determined by the angle of incidence and the energy of the photon. The model used to determine the scattering angle, which is taken from an X-ray database [2], is shown in Fig. 1. This is for an aluminum vacuum chamber surface, but a model for a different surface could be used.

For comparison, we also show in the figure the relative synchrotron radiation spectra for a 2 GeV beam in an arc dipole and a wiggler at CesrTA. Also shown is a direct measurement [3] of reflectivity at 5° from an aluminum surface made at DAPHNE.

Currently, only specular reflection is included, but diffuse scattering can also be simulated by altering the reflectivity model.

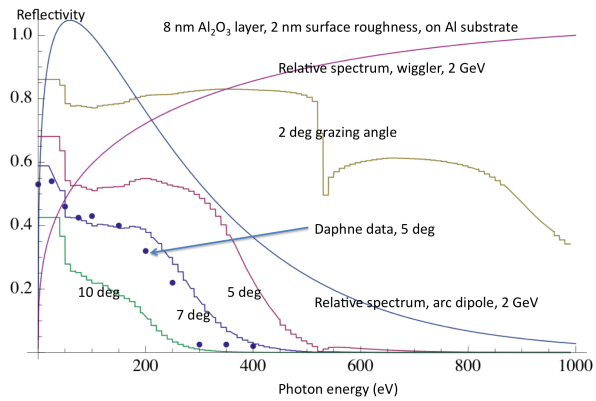

Figure 1: Reflectivity model from LBNL X-ray database

VACUUM CHAMBER MODEL

The vacuum chamber wall is characterized at a number of longitudinal positions by its cross-section. The cross section model is shown in Fig. 2. As shown in the figure, antechambers can be included. A vacuum chamber wall cross-section may also be characterized using a piecewise linear outline.

In between the cross-sections, linear interpolation or triangular meshing can be used. Linear interpolation is faster but is best suited for convex chamber shapes.

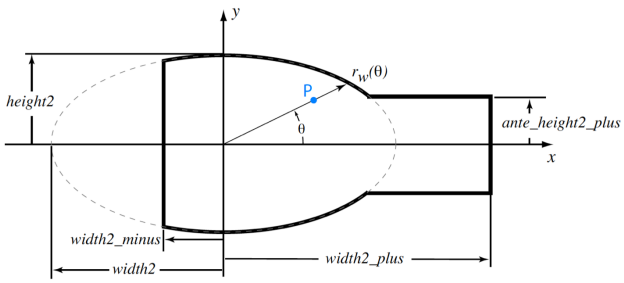

Figure 2: Vacuum chamber model

EXAMPLE 1: PHOTON EMISSION IN A DIPOLE

As the first example, we consider the CesrTA ring with a 5.3 GeV positron beam, and use Synrad3D to simulate photon emission only in the arc dipole at B12W. The vacuum chamber is a simple ellipse. The photons are generated only in the upstream end of this dipole but propagate downstream and can scatter.

In Fig. 3, we show a collection of photon trajectories, projected onto the bend plane. Photons generated by the beam in B12W strike the B12W vacuum chamber a short distance downstream. Some are absorbed here, but most scatter and strike the vacuum chamber further downstream, in B13W. More are absorbed here, but many others scatter again.

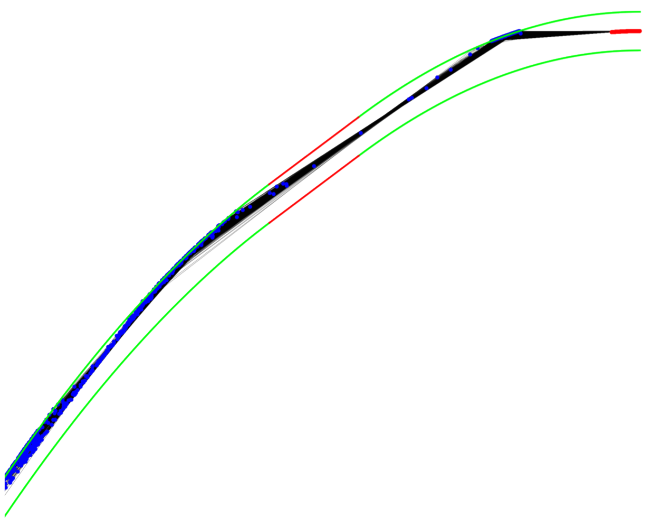

Figure 3: Photon trajectories from B12W: projections onto bend plane. The red dots at the top right are the photon source (the radiating beam in a section of the dipole). Black lines are photon trajectories, and blue dots are photon absorption sites. The upper green lines are the edges of the vacuum chamber in B12W; the red lines are the edges in a straight section, and the lower green lines are the edges of the vacuum chamber in the next dipole, B13W. The geometry has been distorted for purposes of illustration.

These photon trajectories in three dimensions are shown in Fig. 4. Photons from the source (on the right) propagate and strike the vacuum chamber. Blue dots represent absorption sites. For this simple example, in which the photon source is localized longitudinally, the absorption site locations tend to be clumped in several clusters, with decreasing intensity as we get further from the source.

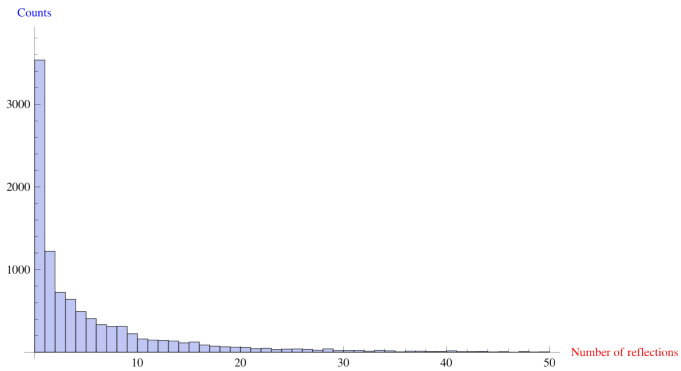

Figure 5: Reflection distribution. The mean number of reflections is 5.4

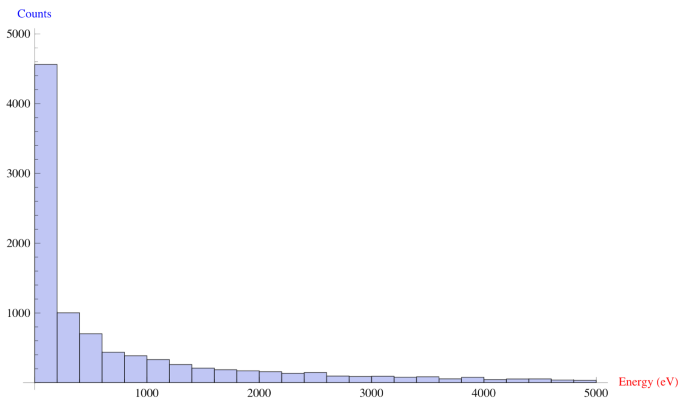

Figure 6: Energy distribution

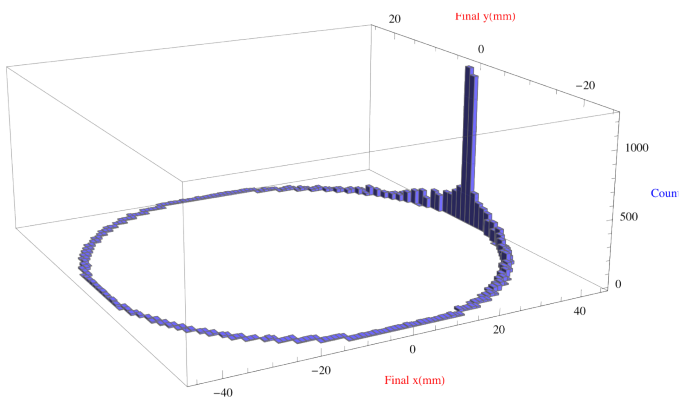

Figure 7: Distribution of photon absorption sites around the vacuum chamber perimeter

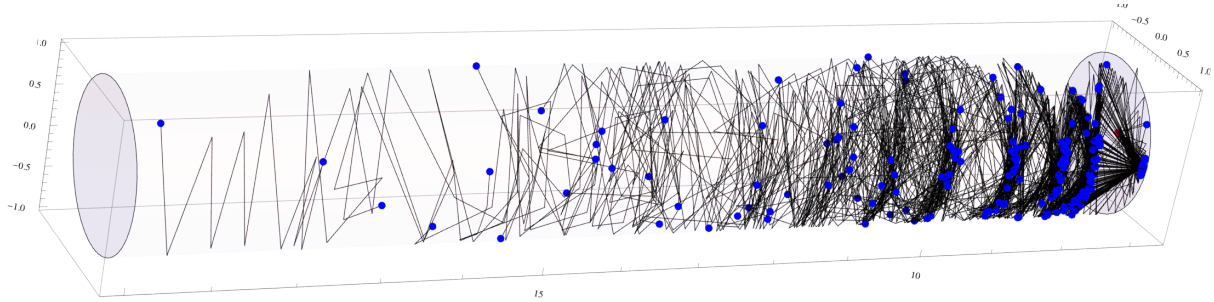

Figure 4: Photon trajectories from B12W in three dimensions. The photon source is on the right. Black lines are trajectories, and blue dots are photon absorption sites. The transverse geometry has been distorted from an ellipse to a circle, and the longitudinal dimension has been rectified and divided by 10, for purposes of illustration.

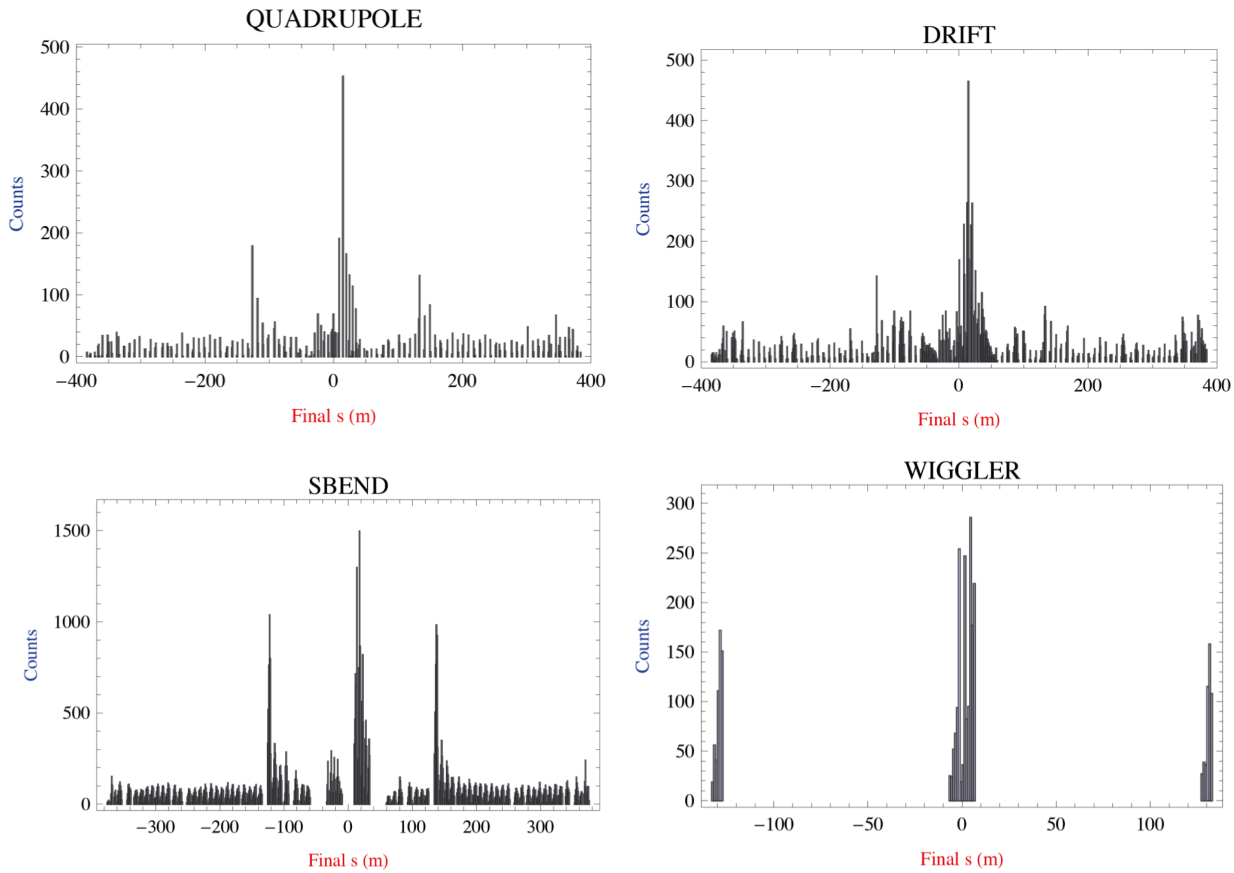

Figure 8: Distribution of photon absorption sites vs. longitudinal position, for different magnetic environments. The origin for the longitudinal coordinate is the center of the L0 straight section. The ring circumference is about 760 m.

Other features of the photon scattering and absorption process are shown in Fig. 5, Fig. 6, and Fig. 7.

In Fig. 5, a histogram of the number of photons, vs. the number of reflections, is presented. Many photons suffer no reflections, that is, they are absorbed as soon as they hit the vacuum chamber, but most are reflected several times before being absorbed. The mean number of reflections is 5.4.

In Fig. 6, a histogram of the number of photons, vs. photon energy, is presented. This is strongly peaked at zero but has a long tail out to at least 5 keV.

In Fig. 7, a two dimensional histogram of the number of photons, vs. location of the absorption site on the vacuum chamber perimeter, is presented. This is is peaked at the outside edge of the vacuum chamber, where the direct photon strikes occur, but there is long tail extending around the entire surface of the vacuum chamber, due to the reflected photons.

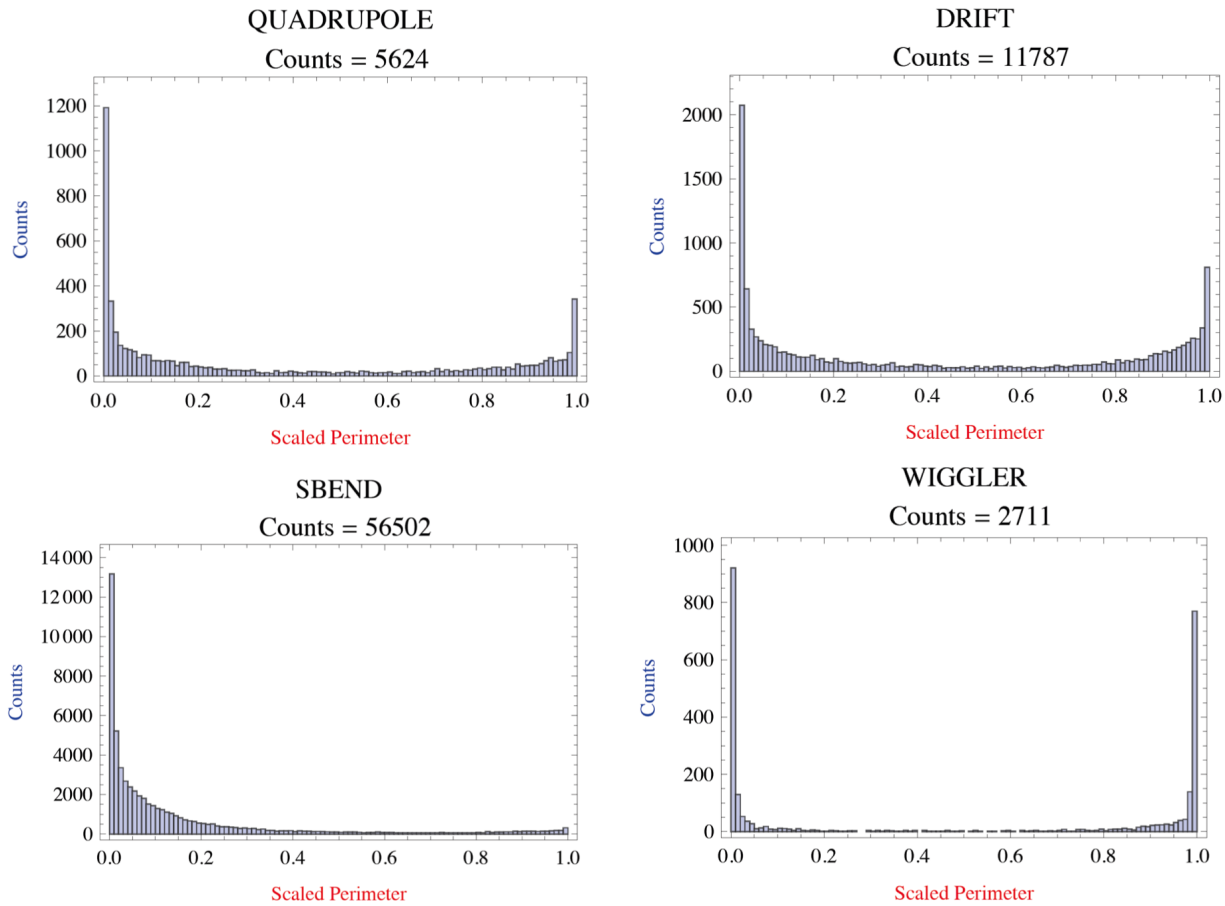

Figure 9: Distribution of photon absorption sites vs. scaled perimeter along the vacuum chamber, for different magnetic environments. The scaled perimeter coordinate varies from zero at the radial outside edge of the vacuum chamber, to 1 at the radial inside edge. Top-bottom symmetry is assumed.

EXAMPLE 2: PHOTON EMISSION THROUGHOUT THE RING

For the second example, photon emission throughout the CesrTA ring from a 2.1 GeV positron beam is simulated. The vacuum chamber is again a simple ellipse.

In Fig. 8, the distribution of photon absorption sites around the ring is shown, sorted by the type of magnetic environment in which the absorption occurs. This information is important for simulations of electron cloud growth, which is strongly influenced by the magnetic environment.

The wigglers in the L0 straight section are responsible for the large peaks in the longitudinal region near $s = 0$. The large peaks near $s = \pm 130$ m are due to wigglers in the arcs near these locations. The small peaks in the arcs are due to the regular Cesr dipoles.

In Fig. 9, we see the distribution of photon absorption sites vs. scaled perimeter along the vacuum chamber, again sorted by the type of magnetic environment in which the absorption occurs.

In the wigglers, most of the photons come from the radiation fans in an upstream wiggler region, so there are strong peaks on both edges of the vacuum chamber. In the bends, most of the radiation is from direct strikes from upstream dipoles, so there is only a strong peak on the radial outside edge, together with a long tail, due to scattering. In the quadrupoles and drifts, there are two peaks, with the higher one at the radial outside, and a distribution between the peaks due to scattering.

SUMMARY

As part of the Bmad software library, a program called Synrad3D has been written to track synchrotron radiation photons generated in storage rings. Synrad3D includes scattering from the vacuum chamber walls using X-ray data from an LBNL database. It can handle any planar lattice and a wide variety of vacuum chamber profiles. Two examples of the application of this program to radiation in CesrTA have been shown and discussed.

REFERENCES

[1] D. Sagan, "Bmad: A relativistic charged particle simulation," Nuc. Instrum. Methods Phys. Res. A, **558**, pp 356-59 (2006)

[2] B.L. Henke, E.M. Gullikson, and J.C. Davis. X-ray interac-

tions: photoabsorption, scattering, transmission, and reflection at E=50-30000 eV, Z=1-92, Atomic Data and Nuclear Data Tables Vol. 54 (no.2), 181-342 (July 1993)

[3] N. Mahne, A. Giglia, S. Nannarone, R. Cimino, C. Vaccarezza, EUROTEV-REPORT-2005-013